

Mini Review

Open Access



Recent progress and perspective of multifunctional integrated zinc-ion supercapacitors

Yue Li¹, Wen Yang², Lu Han^{3,*}, Huijun Li², Zhiguo Wen², Yan Li², Xiaoguang Wang², Hengchao Sun², Ting Lu¹, Min Xu^{1,*} , Likun Pan^{1,*} 

¹Shanghai Key Laboratory of Magnetic Resonance, School of Physics and Electronic Science, East China Normal University, Shanghai 200241, China.

²Beijing Smart-Chip Microelectronics Technology Co., Ltd., Beijing 100192, China.

³Key Laboratory of Spin Electron and Nanomaterials of Anhui Higher Education Institutes, Suzhou University, Suzhou 234000, Anhui, China.

* **Correspondence to:** Prof./Dr. Likun Pan, Shanghai Key Laboratory of Magnetic Resonance, School of Physics and Electronic Science, East China Normal University, Shanghai 200241, China. E-mail: lkpan@phy.ecnu.edu.cn; Prof./Dr. Min Xu, Shanghai Key Laboratory of Magnetic Resonance, School of Physics and Electronic Science, East China Normal University, Shanghai 200241, China. E-mail: xumin@phy.ecnu.edu.cn; Prof./Dr. Han Lu, Key Laboratory of Spin Electron and Nanomaterials of Anhui Higher Education Institutes, Suzhou University, Suzhou 234000, Anhui, China. E-mail: 982563331@qq.com

How to cite this article: Li Y, Yang W, Han L, Li H, Wen Z, Li Y, Wang X, Sun H, Lu T, Xu M, Pan L. Recent progress and perspective of multifunctional integrated zinc-ion supercapacitors. *Energy Mater* 2022;2:200017. <https://dx.doi.org/10.20517/energymater.2022.15>

Received: 15 Apr 2022 **First Decision:** 9 May 2022 **Revised:** 23 May 2022 **Accepted:** 1 Jun 2022 **Published:** 10 Jun 2022

Academic Editor: Yuping Wu **Copy Editor:** Tiantian Shi **Production Editor:** Tiantian Shi

Abstract

Zinc-ion supercapacitors (ZISCs) are recognized as one of the most promising types of energy storage devices with the advantages of high theoretical capacity and safety, nontoxicity, low cost, abundant resources (~300 times higher than lithium), and lightweight. So far, multifunctional integrated ZISCs have greatly broadened their application scenarios. In addition to enhancing the electrochemical performance via the design of advanced electrodes and electrolytes, the complex application scenarios and in-depth development of energy storage devices have resulted in higher requirements for ZISCs with multifunctional integrated applications. However, to the best of our knowledge, there is no relevant review about summarizing advanced multifunctional ZISCs. In this review, various advanced multifunctional ZISCs, including micro, self-powered integrated, antifreezing, and stretchable ZISCs, are comprehensively presented to fully understand the advanced evolution of multifunctional ZISCs. The working principles and challenges of ZISCs are analyzed and the future development directions and expectations of advanced multifunctional ZISCs are discussed. This review provides significant guidance for the multifunctional development of ZISCs for future studies.



© The Author(s) 2022. **Open Access** This article is licensed under a Creative Commons Attribution 4.0 International License (<https://creativecommons.org/licenses/by/4.0/>), which permits unrestricted use, sharing, adaptation, distribution and reproduction in any medium or format, for any purpose, even commercially, as long as you give appropriate credit to the original author(s) and the source, provide a link to the Creative Commons license, and indicate if changes were made.



Keywords: Zinc-ion supercapacitors, energy storage devices, multifunctional integrated applications

INTRODUCTION

Currently, the significant consumption and large-scale demand for energy are major issues prevailing in the world, which are directly related to the economic development of countries and the life quality of their inhabitants^[1-9]. As a result, the utilization of new clean and green energy sources, such as water^[10-13], wave^[14], wind^[15], solar^[16], tidal^[17], biomass^[18], and geothermal energy^[19], has attracted significant attention but still presents problems associated with direct storage, transportation, and instability. Lithium-ion batteries (LIBs) and supercapacitors (SCs) are 2 kinds of widely used energy storage devices. Commercial LIBs show high energy density, stable voltage output, and excellent cycling performance, and operate based on Li⁺ intercalation and deintercalation into and from the electrodes, respectively^[20-24]. However, the irreplaceable toxic organic electrolytes and high cost of lithium limit the applications of LIBs, especially for applications that urgently require high power density^[25-28]. In contrast, SCs are emerging because of their simple preparations, high power densities, and fast charge/discharge rates^[29-32]. The energy storage mechanism of SCs is based on ion adsorption/desorption on the electrode surface without involving the redox reactions in the lattices of the electrode materials, resulting in fast charge/discharge rates and excellent cycling stability, different from that of batteries^[33-36].

At present, by combining the two different energy storage mechanisms of batteries and SCs, the development of hybrid ionic SCs (HISCs) has been promoted, which inherit the high energy density from batteries and the high power density from SCs^[37-41]. HISCs mainly include Li-, Na- and K-ion HISCs assembled with battery-type anodes and capacitive-type cathodes, where the adsorption/desorption of cations occurs on the surface of the cathode with a large specific surface area and abundant active sites, and the exfoliation/deposition of anions (Li⁺, Na⁺ and K⁺) occurs on the anodes to store electrical energy. Unfortunately, lithium, sodium, and potassium metals are required as anodes for necessitating the use of usually toxic organic electrolytes to assemble HISCs^[42-47]. High costs, reactive metal anodes, and toxic and environmentally unfriendly organic electrolytes have limited the development of these monovalent alkali metal-ion HISCs.

Researchers have found several unique advantages for the fast charge transfer kinetics of HISCs based on multivalent ions (Zn²⁺, Ca²⁺, Mg²⁺ and Al³⁺) with abundant reserves and relative safety^[48-52]. Among them, zinc-ion supercapacitors (ZISCs) are recognized as highly promising potential energy storage devices, owing to the high theoretical capacity (823 mAh g⁻¹ and 5855 mAh cm⁻³) of Zn and their high safety, nontoxicity, low cost, abundant resources (~300 times higher than lithium), and lightweight^[53-60]. Furthermore, safe and low-cost aqueous electrolytes can be used in ZISCs. As reported previously, electrical double-layer capacitive- or pseudocapacitive-type electrode materials (such as carbon^[61-67], MXenes^[68-72], conductive polymers^[73-78], and transition metal compounds^[79-84]) are often used as the cathodes of ZISCs, where the typical adsorption/desorption of ions occurs on the electrode surface^[85]. The anodes (Zn and Zn-modified metals) are always dominated by the stripping/plating of ions^[86]. In addition to the low cost of ZISCs, the Zn²⁺/Zn redox on anodes requires two electrons, resulting in a high theoretical volumetric capacity of 5855 mAh cm⁻³, which is beneficial for volume-constrained applications^[87]. Moreover, the equilibrium potential of Zn is -0.76 V vs. a standard hydrogen electrode, illustrating the feasibility of using Zn metal in aqueous electrolytes. Furthermore, compared with other multivalent-ion (Mg²⁺ and Al³⁺) SCs using aqueous electrolytes, ZISCs exhibit faster charge-discharge rates due to the smaller radius of the hydrated ion and faster ionic kinetics^[88]. These advantages push forward the rapid development of ZISCs.

Since the early work on ZISCs reported by Kang and co-workers in 2018^[89], researchers have engaged in boosting the electrochemical performance of ZISCs through the regulation of electrodes and the improvement of the interfacial contact between the electrode and electrolyte. In addition, the rapid development of flexible electronics and multifunctional devices, such as smart skins, energy collectors, wearable electronics, and health monitors, has posed more challenges for the multi-functionalization of ZISCs, like bending, folding, twisting, and stretching, while maintaining their inherent electronic and structural properties^[90]. Simultaneously, multifunctional ZISCs have also been developed towards the merits of lightweight, miniaturization, environmental protection, intelligence, and adaptability at low temperature, with the aim of achieving electronic equipment with full flexibility. In this review, we summarize the recent progress on multifunctional ZISCs, including micro, self-powered integrated, antifreezing, and stretchable ZISCs, as shown in [Figure 1](#)^[91-97]. Moreover, the current challenges and future prospects of multifunctional ZISCs are also described.

Micro-ZISCs

Current research into micro-energy storage components is driven by the development of miniaturized electronic products, such as wearable devices, implantable electronics, and wireless sensor networks^[91,98,99]. Micro-energy devices (micro-SCs and micro-batteries) are regarded as promising candidates. Although the energy density of micro-SCs is smaller than that of micro-batteries, micro-SCs with a similar energy storage mechanism to SCs exhibit faster discharge/charge rates and longer cycling lifetime, thereby representing the optimal choice for practical applications. The main difference between micro-SCs and SCs is their size. The size of the former (only a few square millimeters) is much smaller than that of the latter and is therefore more suitable for the application of implantable electronics, wearable electronics, and other special application scenarios. Furthermore, micro-SCs are usually interdigital, which facilitates the utilization of the effective area of the electrodes, and their specific capacitances are usually measured in the units of $F\text{ cm}^{-2}$ due to their small sizes.

As an important part of the micro-SC family, micro-ZISCs have attracted significant research interests. Zhang *et al.* demonstrated a micro-ZISC with ultrahigh surface energy density and long-term durability by employing activated carbon as a cathode and electrodeposited Zn nanosheet as an anode in a ZnSO_4 -based aqueous electrolyte, which showed a high areal capacitance of 1200 mF cm^{-2} in a voltage window of 0.5-1.5 V with a total size of $1.8 \times 1.8\text{ cm}^2$ ^[100]. Li *et al.* designed a smaller micro-ZISC (with a thickness of $0.851\text{ }\mu\text{m}$) coupled with a $\text{Ti}_3\text{C}_2\text{T}_x$ cathode using a low-cost laser-writing manufacturing route, which displayed a maximum areal capacitance of 72.02 mF cm^{-2} at a scan rate of 10 mV s^{-1} ^[101]. However, the energy density of the reported micro-ZISC was limited by the tight layer-to-layer space. Cheng and co-workers^[102] synthesized one-dimensional (1D) core-shell conductive nanofibers via bacterial cellulose fiber (BCF) and polypyrrole (PPy) as the intercalation species to expand the space of the MXene layers (MXene/BCF@PPy), exhibiting an areal capacitance of 388 mF cm^{-2} . Furthermore, micro-ZISCs using the MXene/BCF@PPy cathodes showed an outstanding energy density of $145.4\text{ }\mu\text{Wh cm}^{-2}$ and excellent capacity retention of 95.8% after 25000 cycles. For aqueous electrolyte-based micro-ZISCs, three key factors for the electrode materials should be considered in the micromanufacturing process: (1) specific surface area; (2) mass loading and size of electrodes; and (3) inherent conductivity. In the micro-application process, the small voltage window limited by hydrogen evolution should also be considered, which is similar to normal ZISCs.

Although the aqueous electrolytes for micro-ZISCs display the merits of low cost, safety, and environmental friendliness, they can cause leakage and be unsuitable for implantable and wearable power sources. Quasi-solid-state electrolytes have similar advantages to aqueous electrolytes, where the electrolytes are solid but still contain some water, thereby avoiding the risk of easy leakage associated with aqueous electrolytes. They act as promising candidates for quasi-solid-state (QSS) micro-ZISCs. Hydrogels, with a 3-dimensional (3D)

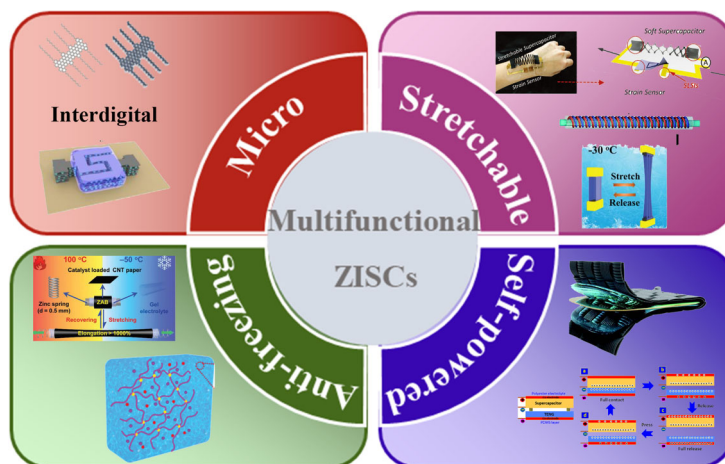


Figure 1. Classification of multifunctional ZISCs, including micro-, self-powered integrated, antifreezing, and stretchable ZISCs. Reproduced with permission from Ref.^[91] (Copyright 2022, Wiley-VCH), Ref.^[92] (Copyright 2021, Elsevier), Ref.^[93] (Copyright 2022, Wiley-VCH), Ref.^[94] (Copyright 2021, Royal Society of Chemistry), Ref.^[95] (Copyright 2021, Royal Society of Chemistry), Ref.^[96] (Copyright 2019, Wiley-VCH) and Ref.^[97] (Copyright 2021, Elsevier).

network structure of polymers containing a large amount of water, are often used as the electrolytes for QSS micro-ZISCs. Moreover, their adjustable shape makes it possible for them to meet the demands of micro-ZISCs. Furthermore, some hydrogels are derived from natural polymers with excellent biocompatibility, flexibility, and environmental friendliness, highlighting their application for QSS micro-ZISCs in flexible and wearable devices.

Cao *et al.* constructed $\text{Zn}(\text{CF}_3\text{SO}_3)_2/\text{polyacrylamide}$ (PAM) electrolyte for micro-ZISCs based on a BCF-intercalated MXene cathode (MXene/BCF) and a zinc anode by laser cutting^[92]. The optimal configuration of the MXene/BCF cathode and the inhibition of the hydrogen and oxygen evolution reactions by the gel electrolyte increase the voltage window to 1.2 V. Using the same electrodes, the surface energy density increased significantly to 34 Wh cm^{-2} compared with the traditional $\text{H}_2\text{SO}_4/\text{PAM}$ hydrogel electrolyte ($0.6 \text{ V}/8.6 \text{ Wh cm}^{-2}$). Tian *et al.* developed novel implantable and biodegradable transient micro-ZISCs using a Zn@PPy cathode by printing a $\text{NaCl}/\text{agarose}$ gel electrolyte and a zinc anode [Figure 2A]^[103]. The assembled micro-ZISC is biodegradable, thereby preventing the waste of materials. As shown in Figure 2C, the XRD pattern of Zn@PPy showed a broad peak at 25° , indicating that the PPy was polymerized successfully on the zinc metal. Benefiting from the short ion transport channel and fast ion transport rate of the 3D interdigitated structure of the electrodes and electrolyte configuration, the assembled micro-ZISC displays an area of only $1 \times 1.4 \text{ cm}^2$ [Figure 2B] with a high energy density of $0.394 \text{ mWh cm}^{-2}$. More importantly, it can be implanted into subcutaneous region of rats and completely degraded within 30 d [Figure 2D-I], accompanied by unimportant changes in cell viability [Figure 2J and K].

Although their energy density is lower than those of batteries and ordinary ZISCs, micro-ZISCs still possess some inherent advantages, such as longer working time (> 100000 cycles), faster charge/discharge rates, and higher power densities, on account of their smaller sizes and shorter electron transport distances. These characteristics endow micro-ZISCs with potentially unique advantages for applications in miniature sensor networks, nanorobots, microelectromechanical systems, and wearable and implantable electronics. In particular, implantable and wearable micro-ZISCs with stable performance and good safety can be readily used as energy storage and power supply units in various human-related experiments. At present, the development of micro-ZISCs is still in an early stage, and there are still many problems to be solved. In

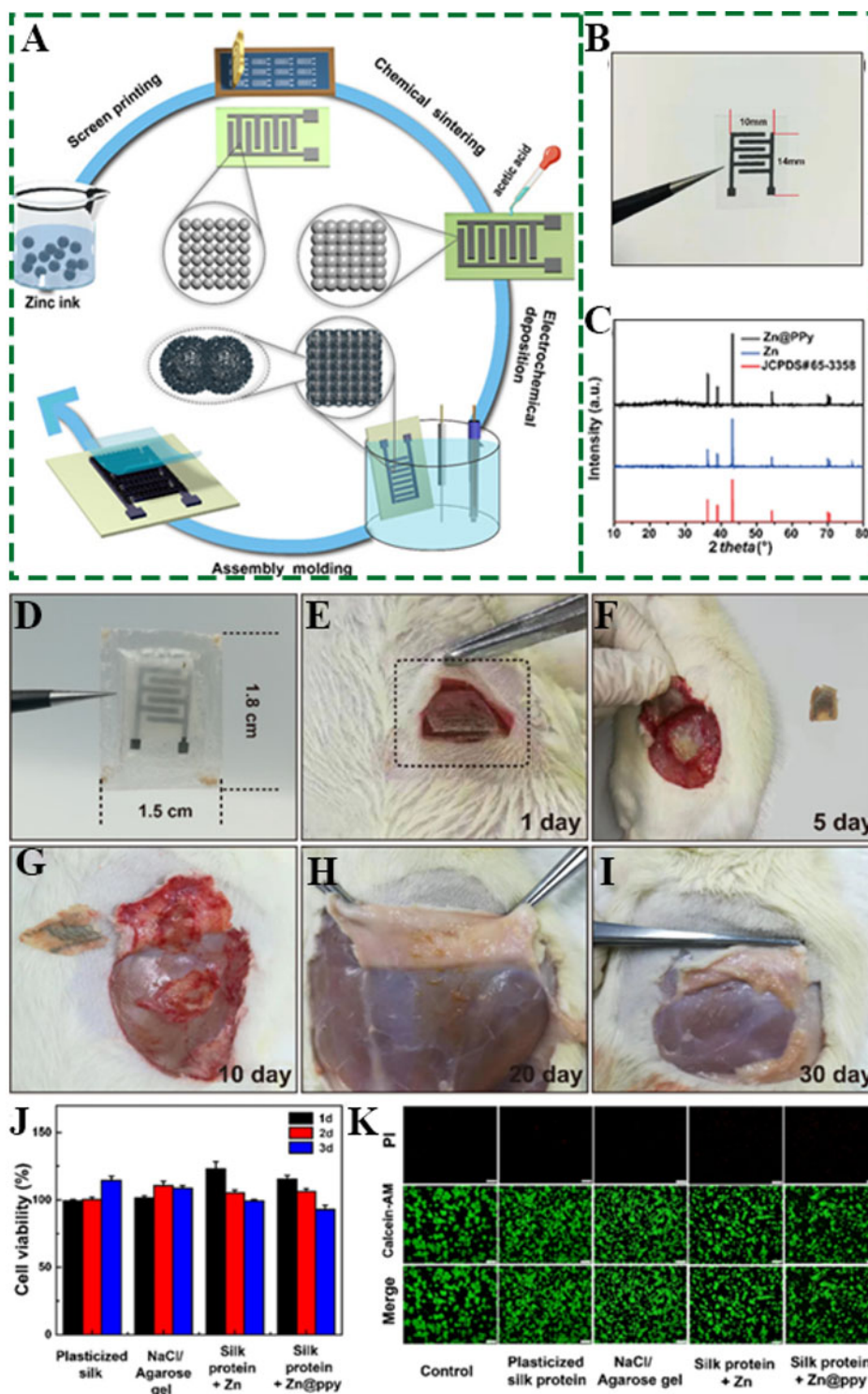


Figure 2. (A) Schematic of super-assembly fabrication processes of a fully biodegradable micro-ZISC, including screen printing, electrochemical sintering, electrochemical deposition, and device assembly. (B) Photograph of micro-ZISC. (C) XRD patterns of Zn and Zn@ppy. (D) Optical images of silk-encapsulated micro-ZISC before implantation. (E-I) *In-vivo* degradation evaluation of micro-ZISC device after being implanted in the subcutaneous region of rats. (J) Cell viability of plasticized silk films, NaCl/agarose gel, silk protein-Zn and silk protein-Zn@ppy films. (K) Fluorescent images showing cell viability, with green (calcein-AM) and red [propidium iodide (PI)] representing live and dead RAW264.7 cells, respectively.^[103] Reproduced with permission from Ref.^[103] (Copyright 2021, American Chemical Society).

terms of performance, advanced electrode materials with high energy densities and electrolytes with fast ion transport rates are urgently needed to improve the overall electrochemical performance of micro-ZISCs. The interdigitated type is the main structure of current micro-ZISCs. Therefore, exploiting more micro-ZISCs with other structures, such as linear and 3D structures, to meet more application scenarios is an important future development direction of micro-ZISCs.

Stretchable ZISCs

In recent years, the rise of flexible devices has promoted the prosperous development of artificial organs, electronic skin, health monitoring, and soft robots^[93,104-106]. As energy sources, batteries and SCs are required to be flexible and wearable to adapt to the inevitable limb movement of the human body in daily activities. Stretchability is another fundamental prerequisite. However, the development of stretchable flexible energy storage devices is limited by the mismatched interface caused by the slippage and fracture between electrodes and electrolytes when tensile deformation occurs. This irreversible mechanical loss and limited interfacial matching are primary factors that restrict the development of flexible energy storage devices. The structure of inchoate stretchable energy storage devices is usually composed of a stretchable hydrogel electrolyte and rigid electrode-based carbon cloth, nickel foam, copper foil, and other fixed-shaped substrates^[6]. Thus, the breakthrough of this restricting factor is to study integrated stretchable energy storage devices. Furthermore, the electrodes and electrolytes should all be stretchable to realize an "all-in-one" design by the development of advanced stretchable ZISCs.

The structural design of electrodes, including spring-like, wave-like, bridge-island, and cellular structures, is one of the most feasible approaches to fabricating integrated stretchable SCs. From the perspective of device dimensions, 1D fiber-like and 2-dimensional (2D) plane-like electrodes play prominent roles in the application of stretchable ZISCs. Among them, 1D fiber-like electrodes can be appropriately rotated into spring-like structures with different stretch lengths through the number of turns and densities. Moreover, 1D fiber-like electrodes can also be woven into stretchable fabrics of various shapes, such as honeycomb and knitted fabrics. 2D-structured electrodes are ultrathin and ultralight and can be expediently integrated into microelectronic devices to form wrinkled or wavy-like stretchable structures to meet the requirements of wearable ZISCs. Lu and co-workers spiraled two parallel wet-spun graphene oxide/carbon nanotube (rGO/CNT) hybrid yarns into spring-like SCs that could be stretched up to 1800%^[107]. Peng and co-workers found that a coaxially arranged structure produced an order of magnitude higher specific capacitance than a parallel arranged structure for spring-like SCs^[108]. Therefore, ultralong coaxial ZISCs with a $\text{Ti}_3\text{C}_2\text{T}_x$ MXene fiber core (cathode) and a zinc fiber shell (anode) were fabricated by a simple wet spinning method. The ZISCs were then enwound into a spring-like structure and woven into a knitted fabric structure, thereby providing stretchability at both the fiber and fabric levels [Figure 3A-D]. The manufactured coaxial ZISCs showed excellent cycling stability with a high area capacitance (up to 214 mF cm^{-2}) and energy density ($42.8 \mu\text{Wh cm}^{-2}$) at 5 mV s^{-1} and an 83.58% capacity retention after 5000 cycles^[99]. Li *et al.* adhered a flat CNT film electrode to the surface of a pre-stretched 700% hydrogel electrolyte through hydrogen bonding^[109]. When the stress dissipated, the CNT film electrode contracted naturally into a wave shape as the hydrogel electrolyte was restored. The strain rate of the ZISCs was determined by the initial pre-stretch ratio of the hydrogel.

Although the structural design of stretchable electrodes can be used to achieve the overall stretchability of ZISCs, the slippage and deformation at the interface of electrode and electrolyte are major contributors to the spoilage of capacity. Therefore, it is crucial for the electrodes to be grown *in situ* on the electrolyte surface. Jin *et al.* proposed the one-step *in situ* growth of a polyaniline (PANI) electrode in an antifreezing organic hydrogel polyelectrolyte based on a mixed solvent of an ethylene glycol (EG)/water-impregnated PAM network, which provided a concept for the *in situ* growth of integrated stretchable ZISCs without

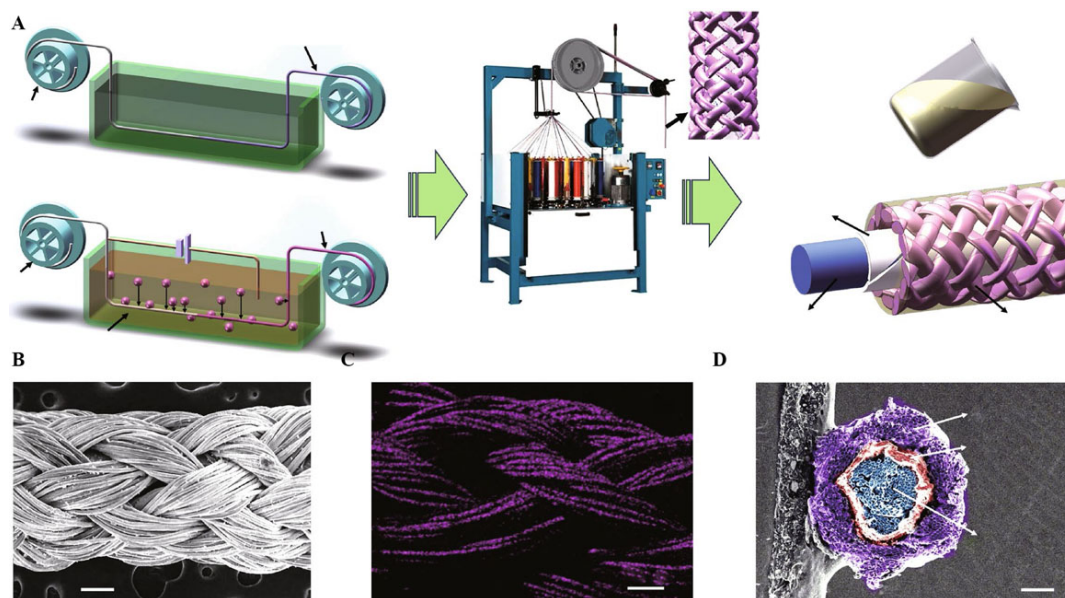


Figure 3. (A) Schematic illustration of large-scale production of MXene- and zinc-coated fibers and braided coaxial ZISCs. (B) SEM image of ZISCs. (C) Mapping image of zinc element on the surface of ZISCs. (D) Cross-sectional SEM image of a coaxial ZISC^[99]. Copyright 2022, Springer.

interfacial mismatching problems^[95]. The complete contact of the PANI electrode and hydrogel electrolyte reduced the interfacial resistance of ion transport in the ZISCs. In addition, the *in situ* synthesis of the rod-like PANI electrode fixed on the surface of the hydrogel electrolyte without deformation and slippage when being stretched resulted in a stable and ultralong cycling performance. In addition to the excellent performance of the all-in-one stretchability, the hydrogel was also endowed with outstanding antifreezing properties due to the addition of EG. The capacitance retained 91.3% of the initial value after 100000 cycles at -30 °C. Density functional theory (DFT) calculations proved that the binding energy between water and EG (-4.86 kcal mol⁻¹) was lower than that between water molecules (-3.74 kcal mol⁻¹). Additionally, the EG/water mixture held stronger interactions (-23.15 kcal mol⁻¹) with the PAM chains than pure water or EG (-9.68 or -4.98 kcal mol⁻¹, respectively). These results indicate that the free water was firmly fixed in the structure of the hydrogel to avoid the hydrogen and oxygen evolution reactions of free water in a wider potential window.

Despite the above work, the *in situ* growth of active materials on the surface of hydrogels is difficult due to their specificity (e.g., swelling, liquid and material penetration). Moreover, it is also difficult to ensure that the active material grown *in situ* is also an uninterrupted surface during stretching. Nevertheless, this strategy is still promising for constructing stretchable ZISCs.

Self-powered integrated ZISCs

Although researchers are working to improve the energy density, power efficiency and service lifetime of various energy storage devices, including SCs and batteries, some pivotal questions still exist. For example, what should we do if the stored electrical energy is used up? For practical applications, ZISCs often need to be charged by an external power source, which is rigidly cumbersome with a distinctly increased volume that reduces the flexibility, industrialization, and miniaturization of ZISCs. In addition, ZISCs are at risk of breaking down in outdoor environments due to the missing external power sources. These issues illustrate pressing concerns regarding the further application of self-powered integrated ZISCs. At present, there are many known methods to generate electricity through energy capture and conversion from wind, solar and

friction energy and air in nature, which could supply power to energy storage devices with green, safe, and environmentally friendly characteristics. Therefore, the design and integration of self-powered integrated ZISCs have attracted significant attention recently.

The development of photovoltaic solar cells has proved that solar energy can be used as an independent energy-harvesting component. The integration of photovoltaic solar cells and SCs can realize the self-charging of SCs without an external power source. Some self-powered lithium-ion SCs (LISCs) coupled with solar cells have been developed^[110,111]. However, photovoltaic solar cells and LISCs require independent and external integration, which increases the floor area of the whole equipment and ohmic transportation loss. The design of a single device architecture represents an optimal route to reach the maximization of efficiency for photovoltaic solar cells and energy storage devices. Therefore, it is necessary to focus on the interfacial effect of various components and explore new materials that are simultaneously suitable for photovoltaic and energy storage applications.

On this basis, Boruah *et al.* demonstrated the first photorechargeable ZISCs using a g-C₃N₄@rGO@FTO photocathode for both solar energy harvesting and energy storage^[112]. g-C₃N₄@rGO@FTO generated photoelectrons in the excited state under the irradiation of light, which were easily transferred to the anode along the external circuit to promote the deposition of Zn²⁺ [Figure 4A]. In contrast, the vacancies adsorbed anions (SO₄²⁻) in the electrolyte and promoted their uniform arrangement on the electrode surface for forming an electric double layer for the ZISCs [Figure 4B]. Benefiting from the synergistic effect of the photocathode, the capacitance was calculated to be 82% from dark conditions to illumination [Figure 4C]. The specific capacitance of the photorechargeable ZISCs was calculated up to 11377 mF g⁻¹ from Figure 4D and E. Furthermore, the electrochemical stability of the photorechargeable ZISCs was analyzed by cycling tests [Figure 4F-H], which showed a 1.4% potential loss after nine cycles and a 17% potential loss after 20 h. Moreover, the electrochemical performance was ignorable after 500 cycles, resulting from the unknown changes in morphology and the resistance of the photocathode. However, solar cells and ZISCs are separate external integrated components, which increases the bulk and resistive transmission spoilage of the overall device. Moreover, the conversion efficiency of solar cells is low, which also limits their production as power generation devices. Therefore, the design of an integrated framework is the best method for maximizing the energy storage efficiency of photorechargeable ZISCs, and it is of great practical significance to explore new materials for this application.

In addition, air, as an indispensable criterion for human life, fills every corner of our living space. On this basis, Ma *et al.* proposed a highly integrated "air-charging" ZISC system, where ZISCs could be easily and safely charged from the power converted from air energy without an external power supply^[96]. More interestingly, the integrated structural design of air-charging ZISCs avoids the problems of mismatched interfaces. As shown in Figure 4I, the outer layer of the air-charging ZISCs was made of carbon fabric-coated porous carbon@Co₄N (CFC@PC@Co₄N) and bent into a "U" shape (one side for energy harvesting of air charging and one side for energy storage of ZISCs). A zinc-metal electrode in the middle simultaneously acted as an anode for the air-charging devices and ZISCs. PAM was fabricated as the electrolyte for the ZISCs, and a sodium polyacrylate electrolyte served as the electrolyte for the air-charging devices [Figure 4J]. For the air-charging device side, an open circuit voltage was generated between the CFC@PC@Co₄N cathode and the zinc anode under an air atmosphere via the reduction reaction of O₂ + 4e⁻ + 2H₂O → 4OH⁻ and the oxidation reaction of Zn + 4OH⁻ → Zn(OH)₄²⁻ + 2e⁻. The ZISCs were charged rapidly to 88% in 10 min by the air-charging devices. The concept of air-charging ZISCs opens up a new field of integrated systems that ultimately solve the problem of reliable self-charging, i.e., charging batteries and SCs anytime and anywhere. However, the working time of air-charging ZISCs relies on the reduction of

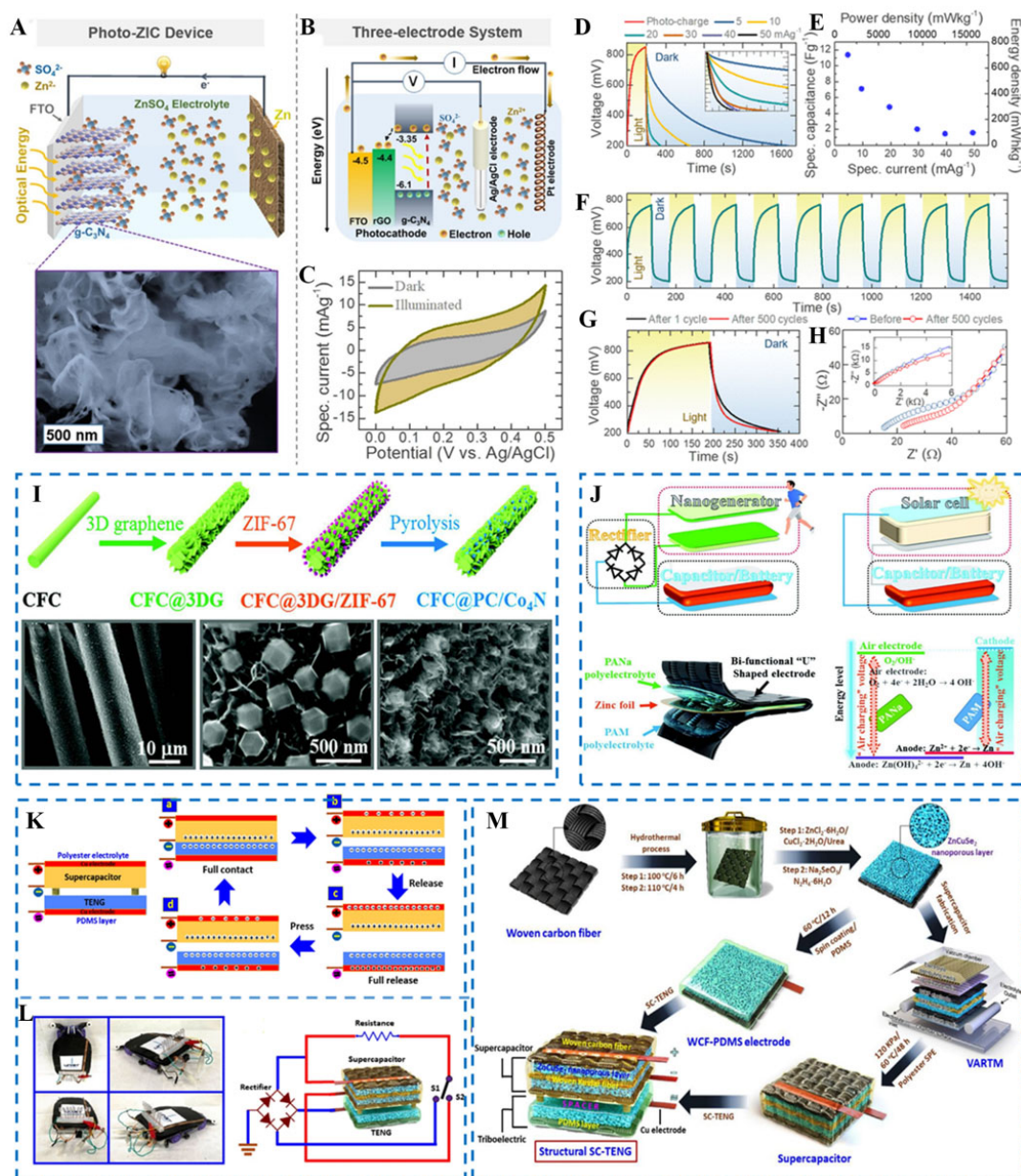


Figure 4. (A) Schematic of 2D $g\text{-C}_3\text{N}_4$ cathode and Zn anode-based photorechargeable ZISCs and SEM image of 2D $g\text{-C}_3\text{N}_4$. (B) Schematic of the 3-electrode experiment of $g\text{-C}_3\text{N}_4@r\text{GO}/\text{FTO}$ electrodes. (C) CV profiles (10 mV s^{-1}) in dark and illuminated conditions ($\lambda\text{-}420\text{ nm}$ and intensity $\text{-}50\text{ mW cm}^{-2}$). (D) Photocharge ($\lambda\text{-}420\text{ nm}$ and intensity $\text{-}50\text{ mW cm}^{-2}$) and discharge cycles at different specific currents of 5, 10, 20, 30, 40, and 50 mA g^{-1} . (E) Photocharged specific capacitance, energy density, and power density plots as a function of discharge specific currents of photorechargeable ZISCs. (F) Cyclic photocharge ($\lambda\text{-}420\text{ nm}$ and intensity $\text{-}50\text{ mW cm}^{-2}$) and discharge cycles at a constant specific current. (G) Comparative plots of the first photocharging and after 500 charge-discharge cycles. (H) Nyquist plots of photorechargeable ZISCs before and after 500 charge-discharge cycles^[112]. Copyright 2020, American Chemical Society. (I) Schematic of synthetic procedure of $\text{CFC}@PC/\text{Co}_3\text{N}_4$ electrode. (J) Different architectures among normal nanogenerator and solar cell charging capacitor/battery systems with air-charging ZISCs, where the nanogenerator and solar cell are only in motion (nanogenerator) or under sufficient solar irradiation (solar cell). The air-charging ZISC ensures the integration of devices by the special "U" shape in this work. The upper part of the "U" shape is a solid-state zinc air-charging battery and the lower part is a solid-state ZISC, both of which share the same zinc-foil anode. On charging, "U" shaped cathodes and zinc-metal anodes were connected to the loading or outside circuit^[96]. Copyright 2019, Wiley-VCH. (K) Triboelectric energy generation mechanism of TENG-ZISCs. (L) TENG-SC-embodied car model for a typical application and electronic circuit diagram of multifunctional TENG-ZISCs. (M) Synthesis procedure of ZnCuSe_2 nanoporous material on woven carbon fiber and development of multifunctional device by vacuum-assisted resin transfer molding and spin-coating method^[97]. Copyright 2021, Elsevier.

air by the catalyst cathode, which could be limited by the accumulation of by-products on the surface of the catalyst cathode during the reduction process. Therefore, increasing the surface area and improving the catalytic activity of the cathode catalyst are 2 pivotal strategies to extend the working time of the air-charging components, thereby improving the service life of the overall self-powered ZISCs in the future.

Compared with the above 2 self-charging methods, triboelectric nanogenerators (TENGs) with a smaller size show significant potential in the application of integrated self-power generation devices by converting mechanical energy into electrical energy output. The working mechanism of TENGs can be described as follows: (1) charge transfer occurs between two thin layers of friction materials with different friction polarities to form a potential difference with an internal circuit due to the friction electrification effect; and (2) in the external circuit, electrons, driven by the potential difference, flow between the two electrodes pasted on the back of the triboelectric material layer or between the electrode and ground to balance the potential difference [Figure 4K]. Impressively, walking, body shaking, hand touching, falling raindrops, and other random environmental energy sources can be used as the power sources for TENGs. Therefore, the combination of a TENG and ZISCs (TENG-ZISCs) is a prime candidate for wearable self-powered ZISCs. Deka *et al.* designed a special flexible 3D spacer fabric to be used as a base material for the full integration of TENG-ZISCs, where ZISCs could be charged from the TENG by utilizing the electrical energy generated by human motion, such as finger pressing [Figures 4L and M]^[97]. Furthermore, based on textile systems, Zhao *et al.* assembled TENG-ZISCs to achieve a self-power supply by a coaxial fiber and integrated a monitoring system simultaneously for detecting temperature changes, thereby achieving the integration of self-power generation, energy storage, and detection^[113]. However, the TENG-ZISCs can only collect the mechanical energy generated by the large-scale movement of the human body and cannot work under the static state of the human body. Furthermore, the voltage generated by the irregular movement of the human body is also unstable. Hence, the requirement for special occasions and unstable voltages limit the development of TENG-ZISCs. The improvement of the sensitivity and power generation efficiency of TENGs is a future challenge for such self-powered ZISCs.

Antifreezing ZISCs

In practical application scenarios, the energy density of traditional ZISCs is attenuated seriously in cold environments due to the sharp drop in ionic conductivity for the freezing of aqueous electrolytes, which narrows the application field for ZISCs. Therefore, research into antifreezing ZISCs, with a particular focus on antifreezing electrolytes, has become a hot topic. Based on the fact that water is prone to freezing below zero, the design concept of antifreezing electrolytes is to limit the free water concentration in the electrolyte. It is generally considered that "water-in-salt" and hydrogel electrolytes are the most feasible methods to suppress free water. "water-in-salt" electrolytes are based on high concentrations ($> 20 \text{ mol L}^{-1}$) of salt dissolved in water to break the hydrogen bonds between water molecules and then combine them with the salt ions. However, "water-in-salt" electrolytes are not recommended as antifreezing electrolytes on account of their high cost and increased viscosity, which does not facilitate ion migration and results in a decreased electrochemical performance of the ZISCs at low temperature.

Hydrogels are hydrophilic 3D network structures formed by supramolecular interactions, entanglement, and chemical crosslinking among polymer chains, which can swell rapidly and maintain a large volume of water without dissolving in water. The amount of water absorbed by a hydrogel is closely related to the crosslinking and 3D structure, in which the water concentration can be as low as a few percent or as high as 99%. There are two pragmatic antifreezing strategies for hydrogels. The first is to enhance the strength and number of hydrogen bonds between the hydrogel polymer network and free water to reduce the free water and promote the antifreezing performance of the hydrogel. However, due to the complexity of polymer network regulation and the small applicable temperature range ($> -20 \text{ }^{\circ}\text{C}$) in cold environments, only a few

works have been reported on such antifreezing hydrogels^[114,115]. In addition, the incorporation of antifreezing additives, including salts, natural biomolecules, and organic solvents, is another method to deploy the water-ice phase equilibrium for antifreezing hydrogels that is convenient and feasible.

High-concentration salts are commonly added as antifreezing agents into hydrogels, and this is considered a typical method to improve their frost resistance properties, following a similar principle as salt in water. Xu *et al.* employed a sodium alginate hydrogel with the addition of 3 M ZnSO₄ as the electrolyte to co-assemble a ZISC with an activated carbon cathode and a zinc anode^[116]. The capacity of the ZISC was improved to 200 mAh g⁻¹ because of the strong interfacial interaction between the electrode and electrolyte for the wettability of the alginate hydrogel. Furthermore, the ability to work at low temperatures (-60-60 °C) with long cycling was comprehensively achieved due to the reduced hydrogen bonding interactions of water in the high-concentration hydrogel electrolyte. Although it is well known that high-concentration salts can significantly improve the antifreezing performance of hydrogels, their high cost and viscosity are inevitable disadvantages. Yang *et al.* first found that low-concentration salts, like Zn(ClO₄)₂, could also enhance the antifreezing performance of hydrogel electrolytes for ZISCs^[117]. A schematic of an antifreezing ZISC is shown in Figure 5A, which was fabricated based on a cathode of natural coconut shell-derived activated carbon, a Zn anode and an antifreezing electrolyte consisting of a PVA/MMT/Zn(ClO₄)₂ hydrogel. The mechanism was found by comparing low-concentration ZnSO₄ and Zn(CF₃SO₃)₂ using molecular dynamics simulations, as shown in Figure 5C-F. In the ZnSO₄ and Zn(CF₃SO₃)₂ hydrogels, hydrogen bonding forms only between the H and O atoms of SO₄²⁺ and CF₃SO₃⁻, while in the Zn(ClO₄)₂ hydrogel, hydrogen bonding forms not only between the H and O atoms from the water molecules but also between the H and O atoms of ClO₄⁻. Therefore, more hydrogen bonds consume the free water in the hydrogel, thereby achieving the antifreezing effect of the hydrogel electrolyte with a low-concentration salt. Figure 5B shows the excellent antifreezing properties reflected by the performance of the ZISC with a 98% capacitance retention over 10000 cycles of ZISCs at -20 °C.

Organic auxiliary (ethylene glycol, propylene glycol, glycerol, ether and DMSO) hydrogel electrolytes are the most essential and common approach for obtaining antifreezing performance, resulting from the lower freezing point of organics. Li and co-workers prepared an antifreezing ZISC with PVA/ethylene glycol/Zn(CF₃SO₃)₂ as the electrolyte by a freezing/thawing method, which maintained a specific capacitance of 63.9% and a high coulombic efficiency of ~100% at -15 °C^[118]. Furthermore, using PVA as a polymer network hydrogel, Jiang *et al.* obtained a PVA/glycerol/ZnSO₄ hydrogel with a freezing point of -105.73 °C by adjusting the ratio of water and glycerol^[119]. The ZISCs using a PVA/glycerol/ZnSO₄ electrolyte ensured all-climate operation at -30~80 °C. Liu *et al.* designed a ZISC using PVA/ethylene glycol/Zn(Tf)₂ as the electrolyte, graphene as the cathode, and zinc foil as the anode, which exhibited a capacitance retention of 60.2% at -20 °C and an excellent ionic conductivity of 3.53 mS cm⁻¹ at -40 °C^[120]. However, the addition of organics often reduces the electrical conductivity and affects the electrochemical performance of ZISCs. Therefore, the optimal design of organic-assisted hydrogel SCs is to adjust the ratio of organics and water.

In nature, many organisms have evolved with unique properties to prevent water crystallization in their bodies and survive in environments below 0 °C. For example, the proline accumulated by transgenic tobacco plants ensures their survival in low-temperature environments^[121] and Arctic fish avoid freezing due to the existence of antifreezing proteins (AFPs)^[122]. Raymond *et al.* proposed the mechanism of AFPs in 1977, in which the "adsorption inhibition" theory held that AFPs were adsorbed on the surface of growing ice, which increased the surface area and volume ratio of ice crystals, thereby inhibiting the growth of ice crystals^[123]. Inspired by AFPs, Mo and co-workers prepared supramolecular hydrogel-based polyacrylic acid (PAA), silk fibroin, and β-cyclodextrin, where β-cyclodextrin was adjacent with amino acid molecules on

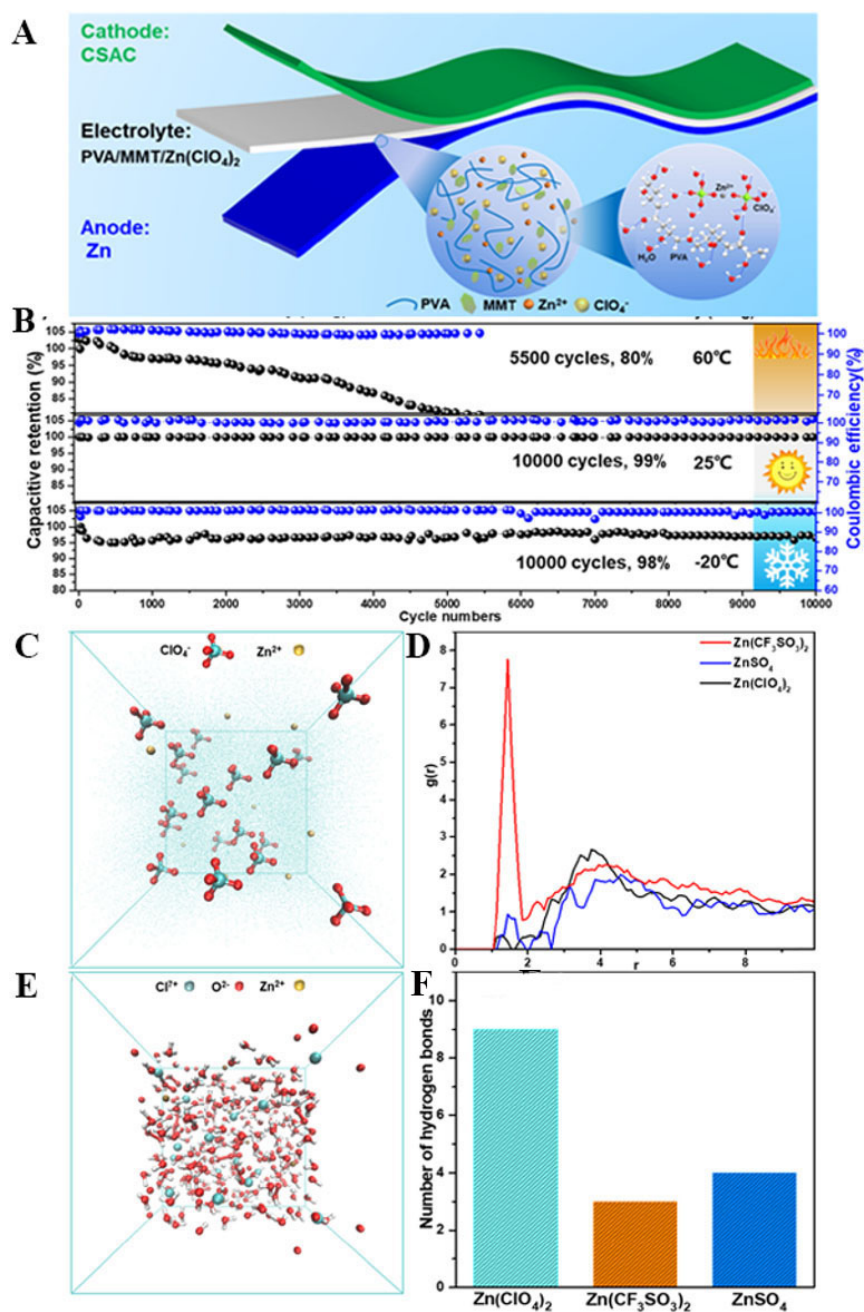


Figure 5. (A) Schematic of QSS CSAC//PVA/MMT/Zn(ClO₄)₂ (gel)//Zn. (B) Cycling performance of QSS ZISC at 5 A g⁻¹ at different temperatures. (C) Molecular dynamics simulation snapshot of Zn(ClO₄)₂ electrolyte. (D) Radial distribution functions of Zn(ClO₄)₂, ZnSO₄ and Zn(CF₃SO₃)₂. (E) Snapshot of molecular dynamics simulation of Zn(ClO₄)₂ and water. (F) Averaged hydrogen bond numbers for Zn(ClO₄)₂, ZnSO₄ and Zn(CF₃SO₃)₂ systems^[117]. Copyright 2021, Elsevier.

the silk fibroin and PAA molecular chain by Schiff base through a host and guest interaction^[124]. Furthermore, the freezing point of the SC fabricated with the supramolecular hydrogel electrolyte was -22.4 to -25.6 °C, lower than that of the PAA hydrogel electrolyte. Compared with salt or organic solvents, AFPs exhibit better biocompatibility, non-toxicity, and environmental friendliness. However, the solubility of AFPs in water is limited and the high concentration of AFPs at low temperatures reduces the ionic conductivity of hydrogels, which greatly restrains their application in antifreezing energy storage devices. In

addition, reducing cost and improving activity are still the major technical problems of AFPs in the future.

In general, the introduction of salts, organic solvents, or AFPs reduces the concentration and activity of free water in electrolytes, which could endow a lower freezing point and antifreezing properties of hydrogel electrolytes, thereby making it possible for applications of ZISCs in low-temperature environments. However, the addition of antifreeze components inevitably increases the electrolyte viscosity, thereby reducing the ion transport rate. Therefore, the development of electrolytes with fast ion transport and stable electrode materials is still a research difficulty for antifreezing ZISCs.

Zn-modified anodes for ZISCs

Commonly, zinc metal (Zn foil or plate) is used as the anode of ZISCs. However, due to the uneven deposition of Zn^{2+} during the stripping/plating process and the side reactions occurring at the interface between zinc metal and an aqueous electrolyte, there are often inevitable zinc dendrites on the surface of the zinc anode, which affect the energy density and safety of ZISCs. Therefore, Zn-modified anodes with a unique surface for Zn^{2+} stripping/deposition are vital to inhibit zinc dendrites. Generally, zinc dendrites could be suppressed by compounding carbon materials on the surface of the zinc plate to adjust the plating/stripping routes of Zn ions at high current density^[125].

Carbon materials with excellent electrical conductivity and large surface areas can provide positive effects for the plating/stripping process of zinc ions on the surface of the Zn anode. Zheng *et al.* defined the crystallography, surface texture, and electrochemical standards of reversible epitaxial electrodeposition and developed a modified Zn anode by electrodepositing graphene on the surface of zinc metal, which employed an epitaxial mechanism to adjust the nucleation, growth, and reversibility of the metal anode^[126]. The low lattice mismatch between graphene and Zn has been proved to effectively drive the deposition of Zn with a locked crystal orientation. This epitaxial Zn anode achieves excellent reversibility for thousands of cycles at medium and high temperatures and provides a preparation expansion method to significantly improve the energy density of ZISCs fabricated by Zn anodes. Li *et al.* synthesized an alkaline MXene-Zn composite (AMX-Zn) for replacing the traditional zinc-foil anode of ZHSCs^[127]. Considering the inevitable stacking and low energy density of 2D carbon materials, Xu *et al.* deposited 3D carbon nanoflowers with O, N-codoped on the surface of a zinc-foil anode for more active sites [Figure 6A and B]^[128]. Furthermore, DFT calculations were used to calculate the binding energy of oxygen and nitrogen doped with zinc atoms and carbon materials to unveil the influence of O and N doping on zincophilic chemistry. Zn tends to bind with oxygen (-3.42 eV), carboxyl oxygen (-0.20 eV), and pyrrole nitrogen (-0.19 eV). Moreover, oxygen shows the strongest binding energy to Zn, which can be explained by its empty antibonding state with the strongest adsorption energy [Figure 6C-E]. Therefore, the carbon nanoflowers on the surface of the zinc anode guided the micrometer-scale hierarchical and uniform deposition of Zn by the rich active sites, which effectively inhibit the production of zinc dendrites.

CONCLUSION AND OUTLOOK

Hybrid ion supercapacitors, which integrate the advantages of supercapacitors (fast charging/discharging speed and high power density) and batteries (high energy density and theoretical capacity), have become emerging and flourishing energy storage devices in recent years. As a branch of ionic supercapacitors, ZISCs have become promising candidates for next-generation energy devices due to their low cost and environmental friendliness. So far, there still exist obstacles to the practical application of ZISCs as high-performance energy storage devices for some specialist scenarios. Therefore, the exploitation of multifunctional ZISCs is crucial to broaden their application range. In this review, we have provided a comprehensive overview of advanced systems for multifunctional ZISCs, including micro-ZISCs (wearable,

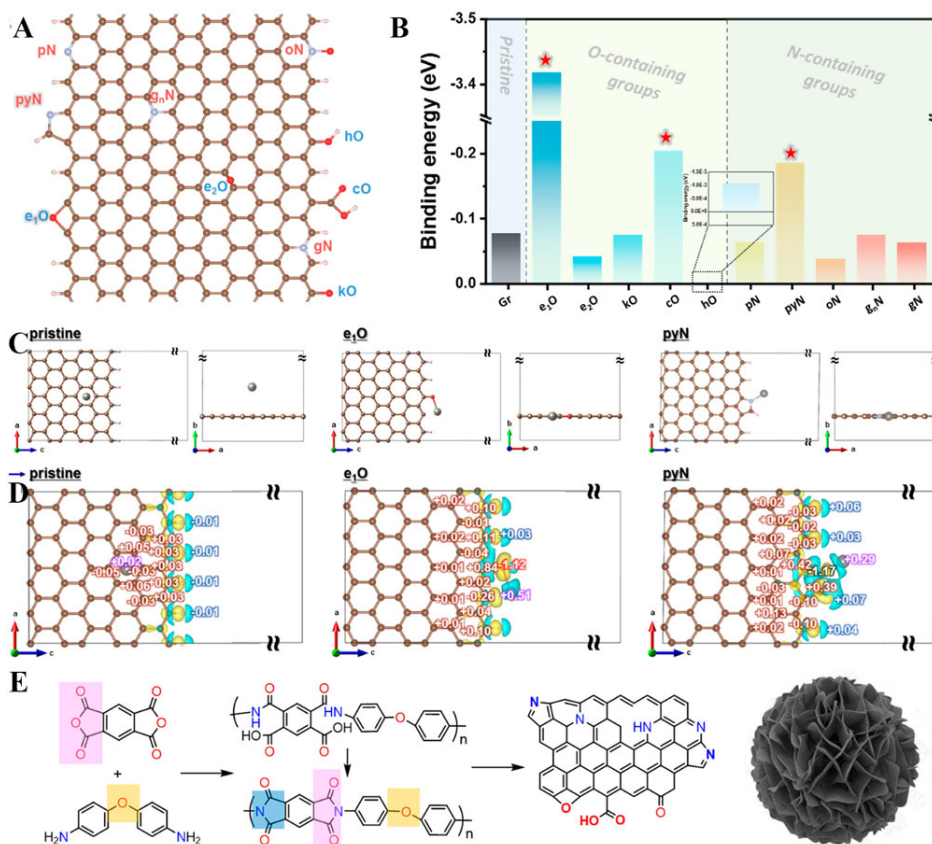


Figure 6. (A) Modeling of oxygen-/nitrogen-doped graphene. (B) Summary of calculated binding energies of Zn atoms with all possible configurations of pristine and O- and N-doped graphene. (C) Model structures for the most stable adsorption sites of Zn atoms. (D) Charge density differences of pristine graphene/Zn, e₁O/Zn and pyN/Zn. (E) Schematic showing the ideal transition from monomers to the polyimide precursor, polyimide, and derived O-/N-codoped carbon^[128]. Copyright 2022, American Chemical Society.

implantable and flexible), self-powered ZISCs (rechargeable without an external power source), antifreezing ZISCs (capable of maintaining a stable working state at low temperature) and stretchable ZISCs (fitting for the stretching and deformation of human skin for wearable devices). In addition, some methods of Zn anode modification for high-performance ZISCs have also been explained. We suppose that the future research on multifunctional ZISCs should consider the following aspects.

For micro-ZISCs, the booming development of portable devices and implantable electronics is devoted to miniaturization, stabilization, industrialization, easy operation, and biocompatibility, which spurs the exploitation of high-performance functional devices. Micro-SCs are considered as promising power supplies with fast charge-discharge rates, adjustable structural design, stability, and high power density. However, the areal energy density of micro-SCs is limited by their small working area ($< 10 \mu\text{Wh cm}^{-2}$). Therefore, the development of micro-ZISCs with capacitive cathodes (high power density) and battery-type anodes (high energy density) has become an evolving trend. More importantly, the typical aqueous electrolytes used in micro-ZISCs further promote the development of safe, inexpensive, environmentally-friendly, and implantable wearable devices. At present, carbon materials dominated by the electric double-layer storage mechanism are mostly used as the cathodes of micro-ZISCs, which require thinner electrode thickness (reducing electrode loading for achieving flexibility) and lead to a lower specific capacity. In addition, the capacity mismatch between capacitor-type cathodes and battery-type anodes is also a bottleneck, restricting the development of micro-ZISCs. For practical applications, micro-ZISCs often demand high

biocompatibility in the fields of implantable and wearable electronics. Therefore, the matching system of high power density cathodes and high energy density anodes with safe biocompatibility should be considered for ideal micro-ZISCs.

Stretchable ZISCs are fabricated by hydrogel electrolytes and stretchable electrodes. Hydrogel electrolytes provide stretchability by dissipating energy through the slipping and breaking of polymer chains during the stretching process. The tensile properties can be adjusted through the characteristic crosslinking mechanism. At present, the strain of hydrogel electrolytes can reach up to 10000%. However, the electrode materials are often inherently non-stretchable. Structural designs, such as spring-, island-bridge- and honeycomb-type shapes, can endow electrodes with stretchability. The strain of electrodes with these structural designs is much lower (1000%) than that of hydrogels. In addition, the interfaces of structurally designed electrodes and hydrogel electrolytes are prone to slip and dislocation during the stretching process, which seriously affects the performance of ZISCs. Therefore, the method by more stable interfacial bonding between electrodes and hydrogel electrolytes, such as the *in situ* growth of electrode materials on the surface of the electrolyte, is the future direction of the development of stretchable ZISCs.

For self-powered ZISCs, many studies have focused on improving the energy density, power density, and self-discharge of ZISCs to improve their service time as power supply devices. However, ZISCs are needed to be charged by an external power supply, which will increase the volume and slow down the process of the wearable industrialization of ZISCs. Therefore, the development of self-powered supercapacitors is essential and remains a huge challenge. As far as generators are concerned, the voltage produced is often low and unstable, which is not possible to fully charge the ZISCs. The inherent stable cycling performance is also limited by the mismatch between the number of charges from the generators. In addition, there are currently only three forms of self-charging ZISCs: triboelectric generators, solar generators, and air charging. Thus, there remains a long way to explore self-charging ZISCs in the future, focusing on the pattern and performance of self-powered functional ZISCs.

The essence of antifreezing ZISCs is the development of antifreezing electrolytes. By introducing salts, organic solvents, or antifreezing proteins into hydrogel electrolytes, they can be endowed with freezing resistance and a certain water retention, thereby expanding the potential applications of hydrogels as flexible electronic materials in low-temperature environments. The research in antifreezing ZISCs is still in its infancy and faces obvious challenges in practical applications, such as the tunable synthesis of antifreezing hydrogel electrolytes, structural design, electronic interconnection, and integrated fabrication. Specifically, the excellent mechanical, electrochemical properties, biological nontoxicity, biocompatibility, and biodegradability of antifreezing hydrogel electrolytes are required for the practical application of flexible electronic devices. Furthermore, the integration between hydrogel electrolytes and electrodes is always poor due to the low modulus and large amount of water in the hydrogels, resulting in low conductivity and poor output performance and interfacial stability of ZISCs. Therefore, new electrode materials should be developed with excellent electrochemical performance to improve the integrated manufacturing process of antifreezing ZISCs.

DECLARATIONS

Authors' contributions

Conceptualization and writing - original draft: Li Y

Writing-review and editing, investigation and supervision: Han L, Xu M, Pan L

Project administration: Lu T

Funding acquisition and visualization: Yang W, Li H, W. Z, Li Y, Wang X, Sun H

Availability of data and materials

Not applicable.

Financial support and sponsorship

We are grateful for financial support of this work from the National Natural Science Foundation of China (21875068) and Fundamental Research Funds for the Central Universities (2020ECNU-GXJC003)

Conflicts of interest

All authors declared that there are no conflicts of interest.

Ethical approval and consent to participate

Not applicable.

Consent for publication

Not applicable.

Copyright

© The Author(s) 2022.

REFERENCES

1. Cui J, Yin J, Meng J, et al. Supermolecule cucurbituril subnanoporous carbon supercapacitor (SCSCS). *Nano Lett* 2021;21:2156-64. [DOI](#) [PubMed](#)
2. Li Y, Zhang J, Chen Q, Xia X, Chen M. Emerging of heterostructure materials in energy storage: a review. *Adv Mater* 2021;33:e2100855. [DOI](#) [PubMed](#)
3. Chen M, Zhang Y, Xing G, Chou S, Tang Y. Electrochemical energy storage devices working in extreme conditions. *Energy Environ Sci* 2021;14:3323-51. [DOI](#)
4. Liu Z, Sato N, Gao W, et al. Demonstration of ultrahigh thermoelectric efficiency of ~7.3% in Mg₃Sb₂/MgAgSb module for low-temperature energy harvesting. *Joule* 2021;5:1196-208. [DOI](#)
5. Song Z, Zhang G, Deng X, et al. Ultra-low-dose pre-metallation strategy served for commercial metal-ion capacitors. *Nanomicro Lett* 2022;14:53. [DOI](#) [PubMed](#) [PMC](#)
6. Han L, Huang H, Fu X, et al. A flexible, high-voltage and safe zwitterionic natural polymer hydrogel electrolyte for high-energy-density zinc-ion hybrid supercapacitor. *Chem Eng J* 2020;392:123733. [DOI](#)
7. Pan G, Li J, Han L, et al. MoS₂ nanosheets with expanded interlayer spacing for ultra-stable aqueous Mg-ion hybrid supercapacitor. *Inorg Chem Front* 2022;9:1666-73. [DOI](#)
8. Chen L, Xu X, Wan L, et al. Carbon-incorporated Fe₃O₄ nanoflakes: high-performance faradaic materials for hybrid capacitive deionization and supercapacitors. *Mater Chem Front* 2021;5:3480-8. [DOI](#)
9. Chen C, Zhao M, Cai Y, et al. Scalable synthesis of strutted nitrogen doped hierarchical porous carbon nanosheets for supercapacitors with both high gravimetric and volumetric performances. *Carbon* 2021;179:458-68. [DOI](#)
10. Dao V, Vu NH, Yun S. Recent advances and challenges for solar-driven water evaporation system toward applications. *Nano Energy* 2020;68:104324. [DOI](#)
11. Dao V, Vu NH, Thi Dang H, Yun S. Recent advances and challenges for water evaporation-induced electricity toward applications. *Nano Energy* 2021;85:105979. [DOI](#)
12. Dao V, Vu NH, Choi H. All day Limnobium laevigatum inspired nanogenerator self-driven via water evaporation. *J Power Sources* 2020;448:227388. [DOI](#)
13. Dao VD. An experimental exploration of generating electricity from nature-inspired hierarchical evaporator: the role of electrode materials. *Sci Total Environ* 2021;759:143490. [DOI](#) [PubMed](#)
14. Tan J, Duan J, Zhao Y, He B, Tang Q. Generators to harvest ocean wave energy through electrokinetic principle. *Nano Energy* 2018;48:128-33. [DOI](#)
15. Liu S, Li X, Wang Y, et al. Magnetic switch structured triboelectric nanogenerator for continuous and regular harvesting of wind energy. *Nano Energy* 2021;83:105851. [DOI](#)
16. Guo Z, Wang J, Wang Y, et al. Achieving steam and electrical power from solar energy by MoS₂-based composites. *Chem Eng J* 2022;427:131008. [DOI](#)

17. Khojasteh D, Lewis M, Tavakoli S, et al. Sea level rise will change estuarine tidal energy: a review. *Renew Sust Energ Rev* 2022;156:111855. DOI
18. Pérez A, Ruiz B, Fuente E, Calvo LF, Paniagua S. Pyrolysis technology for *Cortaderia selloana* invasive species. Prospects in the biomass energy sector. *Renew Energy* 2021;169:178-90. DOI
19. Pokhrel S, Sasmito AP, Sainoki A, et al. Field-scale experimental and numerical analysis of a downhole coaxial heat exchanger for geothermal energy production. *Renew Energy* 2022;182:521-35. DOI
20. Li W, Demir I, Cao D, et al. Data-driven systematic parameter identification of an electrochemical model for lithium-ion batteries with artificial intelligence. *Energy Stor Mater* 2022;44:557-70. DOI
21. Liu H, Xu T, Cai C, et al. Multifunctional superelastic, superhydrophilic, and ultralight nanocellulose-based composite carbon aerogels for compressive supercapacitor and strain sensor. *Adv Funct Materials* 2022. DOI
22. Shekhar A, Parekh M, Pol V. Worldwide ubiquitous utilization of lithium-ion batteries: what we have done, are doing, and could do safely once they are dead? *J Power Sources* 2022;523:231015. DOI
23. Qin W, Zhou N, Wu C, et al. Mini-review on the redox additives in aqueous electrolyte for high performance supercapacitors. *ACS Omega* 2020;5:3801-8. DOI PubMed PMC
24. Xu X, Tang J, Qian H, et al. Three-dimensional networked metal-organic frameworks with conductive polypyrrole tubes for flexible supercapacitors. *ACS Appl Mater Interfaces* 2017;9:38737-44. DOI PubMed
25. Zhang Y, Li J, Gong Z, Xie J, Lu T, Pan L. Nitrogen and sulfur co-doped vanadium carbide MXene for highly reversible lithium-ion storage. *J Colloid Interface Sci* 2021;587:489-98. DOI PubMed
26. Li Y, Liu Y, Wang M, et al. Phosphorus-doped 3D carbon nanofiber aerogels derived from bacterial-cellulose for highly-efficient capacitive deionization. *Carbon* 2018;130:377-83. DOI
27. Xu G, Zhang Y, Gong Z, Lu T, Pan L. Three-dimensional hydrated vanadium pentoxide/MXene composite for high-rate zinc-ion batteries. *J Colloid Interface Sci* 2021;593:417-23. DOI PubMed
28. Xu H, Zhang X, Xie T, et al. Li⁺ assisted fast and stable Mg²⁺ reversible storage in cobalt sulfide cathodes for high performance magnesium/lithium hybrid-ion batteries. *Energy Stor Mater* 2022;46:583-93. DOI
29. Ma Z, Chen J, Vatamanu J, et al. Expanding the low-temperature and high-voltage limits of aqueous lithium-ion battery. *Energy Stor Mater* 2022;45:903-10. DOI
30. Hubble D, Brown DE, Zhao Y, et al. Liquid electrolyte development for low-temperature lithium-ion batteries. *Energy Environ Sci* 2022;15:550-78. DOI
31. Wang X, Su T, Luo Y, et al. Achieving superior lithium storage performances of CoMoO₄ anode for lithium-ion batteries by Si-doping dual vacancies engineering. *Acta Mater* 2022;225:117600. DOI
32. Xu H, Zhu D, Zhu W, et al. Rational design of high concentration electrolytes and MXene-based sulfur host materials toward high-performance magnesium sulfur batteries. *Chem Eng J* 2022;428:131031. DOI
33. Dao V. Comment on "Energy storage via polyvinylidene fluoride dielectric on the counter electrode of dye-sensitized solar cells" by Jiang et al. *J Power Sources* 2017;337:125-9. DOI
34. Wang X, Wang F, Wang L, et al. An aqueous rechargeable Zn//Co₃O₄ battery with high energy density and good cycling behavior. *Adv Mater* 2016;28:4904-11. DOI PubMed
35. Chen P, Yuan X, Xia Y, et al. An artificial polyacrylonitrile coating layer confining zinc dendrite growth for highly reversible aqueous zinc-based batteries. *Adv Sci (Weinh)* 2021;8:e2100309. DOI PubMed PMC
36. He L, Liu Y, Li C, et al. A low-cost Zn-based aqueous supercapacitor with high energy density. *ACS Appl Energy Mater* 2019;2:5835-42. DOI
37. Li B, Dai F, Xiao Q, et al. Nitrogen-doped activated carbon for a high energy hybrid supercapacitor. *Energy Environ Sci* 2016;9:102-6. DOI
38. Zuo W, Li R, Zhou C, Li Y, Xia J, Liu J. Battery-supercapacitor hybrid devices: recent progress and future prospects. *Adv Sci (Weinh)* 2017;4:1600539. DOI PubMed PMC
39. Zhang S, Yin B, Liu X, Gu D, Gong H, Wang Z. A high energy density aqueous hybrid supercapacitor with widened potential window through multi approaches. *Nano Energy* 2019;59:41-9. DOI
40. Xu X, Liu Y, Wang M, et al. Hierarchical hybrids with microporous carbon spheres decorated three-dimensional graphene frameworks for capacitive applications in supercapacitor and deionization. *Electrochim Acta* 2016;193:88-95. DOI
41. Zhang Y, Li J, Ma L, et al. Insights into the storage mechanism of 3D nanoflower-like V₃S₄ anode in sodium-ion batteries. *Chem Eng J* 2022;427:130936. DOI
42. Liu H, Liu X, Wang S, Liu H, Li L. Transition metal based battery-type electrodes in hybrid supercapacitors: a review. *Energy Stor Mater* 2020;28:122-45. DOI
43. Kim E, Kim H, Park BJ, et al. Etching-assisted crumpled graphene wrapped spiky iron oxide particles for high-performance Li-Ion hybrid supercapacitor. *Small* 2018;14:e1704209. DOI PubMed
44. Wang J, Zhang Z, Zhang X, et al. Cation exchange formation of prussian blue analogue submicroboxes for high-performance Na-ion hybrid supercapacitors. *Nano Energy* 2017;39:647-53. DOI
45. Deng W, Wang X, Liu C, et al. Li/K mixed superconcentrated aqueous electrolyte enables high-performance hybrid aqueous supercapacitors. *Energy Stor Mater* 2019;20:373-9. DOI
46. Lim E, Kim H, Jo C, et al. Advanced hybrid supercapacitor based on a mesoporous niobium pentoxide/carbon as high-performance

- anode. *ACS Nano* 2014;8:8968-78. [DOI](#) [PubMed](#)
47. Wan L, Tang Y, Chen L, et al. In-situ construction of g-C₃N₄/Mo₂CT_x hybrid for superior lithium storage with significantly improved Coulombic efficiency and cycling stability. *Chem Eng J* 2021;410:128349. [DOI](#)
 48. Aslam MK, Niu Y, Xu M. MXenes for non-lithium-ion (Na, K, Ca, Mg, and Al) batteries and supercapacitors. *Adv Energy Mater* 2021;11:2000681. [DOI](#)
 49. Gao H, Li Y, Zhao H, Xiang J, Cao Y. A general fabrication approach on spinel MCo₂O₄ (M = Co, Mn, Fe, Mg and Zn) submicron prisms as advanced positive materials for supercapacitor. *Electrochim Acta* 2018;262:241-51. [DOI](#)
 50. Wang Q, Wen Z, Li J. A hybrid supercapacitor fabricated with a carbon nanotube cathode and a TiO₂-B nanowire anode. *Adv Funct Mater* 2006;16:2141-6. [DOI](#)
 51. Molinari A, Leufke PM, Reitz C, et al. Hybrid supercapacitors for reversible control of magnetism. *Nat Commun* 2017;8:15339. [DOI](#) [PubMed](#) [PMC](#)
 52. Qi JL, Lin JH, Wang X, et al. Low resistance VFG-Microporous hybrid Al-based electrodes for supercapacitors. *Nano Energy* 2016;26:657-67. [DOI](#)
 53. Wang H, Ye W, Yang Y, Zhong Y, Hu Y. Zn-ion hybrid supercapacitors: achievements, challenges and future perspectives. *Nano Energy* 2021;85:105942. [DOI](#)
 54. Wang H, Wang M, Tang Y. A novel zinc-ion hybrid supercapacitor for long-life and low-cost energy storage applications. *Energy Stor Mater* 2018;13:1-7. [DOI](#)
 55. Chebrolov VT, Balakrishnan B, Chinnadurai D, Kim H. Selective growth of Zn-Co-Se nanostructures on various conductive substrates for asymmetric flexible hybrid supercapacitor with enhanced performance. *Adv Mater Technol* 2019;5:1900873. [DOI](#)
 56. Xu Y, Chen X, Huang C, et al. Redox-active p-phenylenediamine functionalized reduced graphene oxide film through covalently grafting for ultrahigh areal capacitance Zn-ion hybrid supercapacitor. *J Power Sources* 2021;488:229426. [DOI](#)
 57. Jin J, Geng X, Chen Q, Ren TL. A better Zn-ion storage device: recent progress for Zn-ion hybrid supercapacitors. *Nanomicro Lett* 2022;14:64. [DOI](#) [PubMed](#) [PMC](#)
 58. Yang Y, Chen D, Wang H, et al. Two-step nitrogen and sulfur doping in porous carbon dodecahedra for Zn-ion hybrid supercapacitors with long term stability. *Chem Eng J* 2022;431:133250. [DOI](#)
 59. Li J, Li J, Ding Z, et al. In-situ encapsulation of Ni₃S₂ nanoparticles into N-doped interconnected carbon networks for efficient lithium storage. *Chem Eng J* 2019;378:122108. [DOI](#)
 60. Li J, Qin W, Xie J, et al. Rational design of MoS₂-reduced graphene oxide sponges as free-standing anodes for sodium-ion batteries. *Chem Eng J* 2018;332:260-6. [DOI](#)
 61. Zhao J, Burke AF. Electrochemical capacitors: performance metrics and evaluation by testing and analysis. *Adv Energy Mater* 2021;11:2002192. [DOI](#)
 62. Zhang M, Wang W, Tan L, et al. From wood to thin porous carbon membrane: ancient materials for modern ultrafast electrochemical capacitors in alternating current line filtering. *Energy Stor Mater* 2021;35:327-33. [DOI](#)
 63. Cai P, Momen R, Li M, et al. Functional carbon materials processed by NH₃ plasma for advanced full-carbon sodium-ion capacitors. *Chem Eng J* 2021;420:129647. [DOI](#)
 64. Platek-mielczarek A, Frackowiak E, Fic K. Specific carbon/iodide interactions in electrochemical capacitors monitored by EQCM technique. *Energy Environ Sci* 2021;14:2381-93. [DOI](#)
 65. Zhang M, Dong K, Saeedi Garakani S, et al. Bridged carbon fabric membrane with boosted performance in AC line-filtering capacitors. *Adv Sci (Weinh)* 2022;9:e2105072. [DOI](#) [PubMed](#) [PMC](#)
 66. Hu X, Wang G, Li J, et al. Significant contribution of single atomic Mn implanted in carbon nanosheets to high-performance sodium-ion hybrid capacitors. *Energy Environ Sci* 2021;14:4564-73. [DOI](#)
 67. Chen J, Chen H, Chen M, Zhou W, Tian Q, Wong C. Nacre-inspired surface-engineered MXene/nanocellulose composite film for high-performance supercapacitors and zinc-ion capacitors. *Chem Eng J* 2022;428:131380. [DOI](#)
 68. Ando Y, Okubo M, Yamada A, Otani M. Capacitive versus pseudocapacitive storage in MXene. *Adv Funct Mater* 2020;30:2000820. [DOI](#)
 69. Wen Y, Chen H, Wu M, Li C. Vertically oriented MXene bridging the frequency response and capacity density gap for AC-filtering pseudocapacitors. *Adv Funct Materials* 2022;32:2111613. [DOI](#)
 70. Mainka J, Gao W, He N, Dillet J, Lottin O. A General Equivalent Electrical Circuit Model for the characterization of MXene/graphene oxide hybrid-fiber supercapacitors by electrochemical impedance spectroscopy - impact of fiber length. *Electrochim Acta* 2022;404:139740. [DOI](#)
 71. Li F, Liu Y, Wang G, et al. 3D porous H-Ti₃C₂T films as free-standing electrodes for zinc ion hybrid capacitors. *Chem Eng J* 2022;435:135052. [DOI](#)
 72. Yang B, Liu B, Chen J, et al. Realizing high-performance lithium ion hybrid capacitor with a 3D MXene-carbon nanotube composite anode. *Chem Eng J* 2022;429:132392. [DOI](#)
 73. Cui F, Liu Z, Ma D, et al. Polyarylimide and porphyrin based polymer microspheres for zinc ion hybrid capacitors. *Chem Eng J* 2021;405:127038. [DOI](#)
 74. Wang L, Zhang X, Xu Y, et al. Tetrabutylammonium-intercalated 1T-MoS₂ nanosheets with expanded interlayer spacing vertically coupled on 2D delaminated MXene for high-performance lithium-ion capacitors. *Adv Funct Mater* 2021;31:2104286. [DOI](#)
 75. Yuan T, Luo S, Soule L, et al. A hierarchical Ti₂Nb₁₀O₂₉ composite electrode for high-power lithium-ion batteries and capacitors.

- Mater Today* 2021;45:8-19. DOI
76. Li Z, Zhao L, Zheng X, et al. Continuous PEDOT:PSS nanomesh film: towards aqueous AC line filtering capacitor with ultrahigh energy density. *Chem Eng J* 2022;430:133012. DOI
 77. Sappia LD, Pascual BS, Azzaroni O, Marmisollé W. PEDOT-based stackable paper electrodes for metal-free supercapacitors. *ACS Appl Energy Mater* 2021;4:9283-93. DOI
 78. Feng X, Wang X, Wang M, et al. Novel PEDOT dispersion by in-situ polymerization based on sulfated nanocellulose. *Chem Eng J* 2021;418:129533. DOI
 79. Seo S, Oh I, Park J, et al. Growth of transition metal dichalcogenide heterojunctions with metal oxides for metal-insulator-semiconductor capacitors. *ACS Appl Nano Mater* 2021;4:12017-23. DOI
 80. Hu P, Liu Y, Liu H, Wu X, Liu B. MnCo₂O₄ nanosheet/NiCo₂S₄ nanowire heterostructures as cathode materials for capacitors. *ACS Appl Nano Mater* 2021;4:2183-9. DOI
 81. Gao L, Chen G, Zhang L, Yan B, Yang X. Engineering pseudocapacitive MnMoO₄@C microrods for high energy sodium ion hybrid capacitors. *Electrochim Acta* 2021;379:138185. DOI
 82. Hussain S, Vamsi Krishna B, Nagaraju G, Chandra Sekhar S, Narsimulu D, Yu JS. Porous Co-MoS₂@Cu₂MoS₄ three-dimensional nanoflowers via in situ sulfurization of Cu₂O nanospheres for electrochemical hybrid capacitors. *Chem Eng J* 2021;403:126319. DOI
 83. Ma Y, Xu M, Liu R, et al. Molecular tailoring of MnO₂ by bismuth doping to achieve aqueous zinc-ion battery with capacitor-level durability. *Energy Stor Mater* 2022;48:212-22. DOI
 84. Soltani H, Bahiraei H, Ghasemi S. Effect of electrodeposition time on the super-capacitive performance of electrodeposited MnO₂ on g-C₃N₄ nanosheets. *J Alloy Compd* 2022;904:163565. DOI
 85. Wang S, Li T, Yin Y, Chang N, Zhang H, Li X. High-energy-density aqueous zinc-based hybrid supercapacitor-battery with uniform zinc deposition achieved by multifunctional decoupled additive. *Nano Energy* 2022;96:107120. DOI
 86. Liu P, Fan X, Ouyang B, et al. A Zn-ion hybrid capacitor with enhanced energy density for anode-free. *J Power Sources* 2022;518:230740. DOI
 87. Cao Y, Tang X, Liu M, et al. Thin-walled porous carbon tile-packed paper for high-rate Zn-ion capacitor cathode. *Chem Eng J* 2022;431:133241. DOI
 88. Yi Z, Chen G, Hou F, Wang L, Liang J. Strategies for the stabilization of Zn metal anodes for Zn-ion batteries. *Adv Energy Mater* 2021;11:2003065. DOI
 89. Dong L, Ma X, Li Y, et al. Extremely safe, high-rate and ultralong-life zinc-ion hybrid supercapacitors. *Energy Stor Mater* 2018;13:96-102. DOI
 90. Chao D, Zhou W, Xie F, et al. Roadmap for advanced aqueous batteries: from design of materials to applications. *Sci Adv* 2020;6:eaba4098. DOI PubMed PMC
 91. Liu Z, Hu Y, Zheng W, et al. Untying the bundles of solution-synthesized graphene nanoribbons for highly capacitive micro-supercapacitors. *Adv Funct Mater* 2022;32:2109543. DOI
 92. Cao Z, Fu J, Wu M, Hua T, Hu H. Synchronously manipulating Zn²⁺ transfer and hydrogen/oxygen evolution kinetics in MXene host electrodes toward symmetric Zn-ions micro-supercapacitor with enhanced areal energy density. *Energy Stor Mater* 2021;40:10-21. DOI
 93. Zhu M, Ji S, Luo Y, et al. A mechanically interlocking strategy based on conductive microbridges for stretchable electronics. *Adv Mater* 2022;34:e2101339. DOI PubMed
 94. Gu C, Xie X, Liang Y, et al. Small molecule-based supramolecular-polymer double-network hydrogel electrolytes for ultra-stretchable and waterproof Zn-air batteries working from -50 to 100 °C. *Energy Environ Sci* 2021;14:4451-62. DOI
 95. Jin X, Song L, Yang H, et al. Stretchable supercapacitor at -30 °C. *Energy Environ Sci* 2021; 14:3075-85. DOI
 96. Ma L, Zhao Y, Ji X, et al. A usage scenario independent "air chargeable" flexible zinc ion energy storage device. *Adv Energy Mater* 2019;9:1900509. DOI
 97. Deka BK, Hazarika A, Kwak M, et al. Triboelectric nanogenerator-integrated structural supercapacitor with in situ MXene-dispersed N-doped Zn-Cu selenide nanostructured woven carbon fiber for energy harvesting and storage. *Energy Stor Mater* 2021;43:402-10. DOI
 98. Zhang C, Peng Z, Huang C, et al. High-energy all-in-one stretchable micro-supercapacitor arrays based on 3D laser-induced graphene foams decorated with mesoporous ZnP nanosheets for self-powered stretchable systems. *Nano Energy* 2021;81:105609. DOI
 99. Shi B, Li, Chen A, Jen TC, Liu X, Shen G. Continuous fabrication of Ti₃C₂T_x MXene-based braided coaxial zinc-ion hybrid supercapacitors with improved performance. *Nanomicro Lett* 2021;14:34. DOI PubMed PMC
 100. Zhang P, Li Y, Wang G, et al. Zn-ion hybrid micro-supercapacitors with ultrahigh areal energy density and long-term durability. *Adv Mater* 2019;31:e1806005. DOI PubMed
 101. Liu W, Jiang K, Chen D, Qu F, Shen G. In-situ annealed Ti₃C₂T_x MXene based all-solid-state flexible Zn-ion hybrid micro supercapacitor array with enhanced stability. *Nanomicro Lett* 2021;13:100. DOI
 102. Cheng W, Fu J, Hu H, Ho D. Interlayer structure engineering of MXene-based capacitor-type electrode for hybrid micro-supercapacitor toward battery-level energy density. *Adv Sci (Weinh)* 2021;8:e2100775. DOI PubMed PMC
 103. Tian W, Li Y, Zhou J, et al. Implantable and biodegradable micro-supercapacitor based on a superassembled three-dimensional network Zn@PPy hybrid electrode. *ACS Appl Mater Interfaces* 2021;13:8285-93. DOI PubMed
 104. Mu C, Wang X, Ma Z, Liu X, Li W. Redox and conductive underwater adhesive: an innovative electrode material for convenient

- construction of flexible and stretchable supercapacitors. *J Mater Chem A* 2022;10:7207-17. DOI
105. Kang MS, Heo I, Cho KG, et al. Coarsening-induced hierarchically interconnected porous carbon polyhedrons for stretchable ionogel-based supercapacitors. *Energy Stor Mater* 2022;45:380-8. DOI
 106. Sun Q, Wang L, Ren G, et al. Smart band-aid: multifunctional and wearable electronic device for self-powered motion monitoring and human-machine interaction. *Nano Energy* 2022;92:106840. DOI
 107. Lu Z, Foroughi J, Wang C, Long H, Wallace GG. Superelastic hybrid CNT/graphene fibers for wearable energy storage. *Adv Energy Mater* 2018;8:1702047. DOI
 108. Chen X, Qiu L, Ren J, et al. Novel electric double-layer capacitor with a coaxial fiber structure. *Adv Mater* 2013;25:6436-41. DOI PubMed
 109. Li H, Lv T, Sun H, et al. Ultrastretchable and superior healable supercapacitors based on a double cross-linked hydrogel electrolyte. *Nat Commun* 2019;10:536. DOI PubMed PMC
 110. Tian Z, Tong X, Sheng G, et al. Printable magnesium ion quasi-solid-state asymmetric supercapacitors for flexible solar-charging integrated units. *Nat Commun* 2019;10:4913. DOI PubMed PMC
 111. Paoletta A, Faure C, Bertoni G, et al. Light-assisted delithiation of lithium iron phosphate nanocrystals towards photo-rechargeable lithium ion batteries. *Nat Commun* 2017;8:14643. DOI PubMed PMC
 112. Boruah BD, Mathieson A, Wen B, Jo C, Deschler F, De Volder M. Photo-rechargeable zinc-ion capacitor using 2D graphitic carbon nitride. *Nano Lett* 2020;20:5967-74. DOI PubMed
 113. Zhao J, Cong Z, Hu J, et al. Regulating zinc electroplating chemistry to achieve high energy coaxial fiber Zn ion supercapacitor for self-powered textile-based monitoring system. *Nano Energy* 2022;93:106893. DOI
 114. Zhang D, Liu Y, Liu Y, et al. A general crosslinker strategy to realize intrinsic frozen resistance of hydrogels. *Adv Mater* 2021;33:e2104006. DOI PubMed
 115. Mo F, Liang G, Meng Q, et al. A flexible rechargeable aqueous zinc manganese-dioxide battery working at -20 °C. *Energy Environ Sci* 2019;12:706-15. DOI
 116. Xu Z, Ma R, Wang X. Ultrafast, long-life, high-loading, and wide-temperature zinc ion supercapacitors. *Energy Stor Mater* 2022;46:233-42. DOI
 117. Yang G, Huang J, Wan X, et al. A low cost, wide temperature range, and high energy density flexible quasi-solid-state zinc-ion hybrid supercapacitors enabled by sustainable cathode and electrolyte design. *Nano Energy* 2021;90:106500. DOI
 118. Li Z, Chen D, An Y, et al. Flexible and anti-freezing quasi-solid-state zinc ion hybrid supercapacitors based on pencil shavings derived porous carbon. *Energy Stor Mater* 2020;28:307-14. DOI
 119. Jiang Y, Ma K, Sun M, Li Y, Liu J. All-climate stretchable dendrite-free Zn-ion hybrid supercapacitors enabled by hydrogel electrolyte engineering. *Energy Environ Mater* 2022. DOI
 120. Liu J, Khanam Z, Ahmed S, Wang T, Wang H, Song S. Flexible antifreeze Zn-ion hybrid supercapacitor based on gel electrolyte with graphene electrodes. *ACS Appl Mater Interfaces* 2021;13:16454-68. DOI PubMed
 121. Lv J, Song Y, Jiang L, Wang J. Bio-inspired strategies for anti-icing. *ACS Nano* 2014;8:3152-69. DOI PubMed
 122. He Z, Wu C, Hua M, et al. Bioinspired multifunctional anti-icing hydrogel. *Matter* 2020;2:723-34. DOI
 123. Raymond JA, DeVries AL. Adsorption inhibition as a mechanism of freezing resistance in polar fishes. *Proc Natl Acad Sci U S A* 1977;74:2589-93. DOI PubMed PMC
 124. Mo F, Li Q, Liang G, et al. A self-healing crease-free supramolecular all-polymer supercapacitor. *Adv Sci (Weinh)* 2021;8:2100072. DOI PubMed PMC
 125. Zhang N, Chen X, Yu M, Niu Z, Cheng F, Chen J. Materials chemistry for rechargeable zinc-ion batteries. *Chem Soc Rev* 2020;49:4203-19. DOI PubMed
 126. Zheng J, Zhao Q, Tang T, et al. Reversible epitaxial electrodeposition of metals in battery anodes. *Science* 2019;366:645-8. DOI PubMed
 127. Li Z, Guo D, Wang D, Sun M, Sun H. Exploration of Metal/Ti₃C₂ MXene-derived composites as anode for high-performance zinc-ion supercapacitor. *J Power Sources* 2021;506:230197. DOI
 128. Xu Z, Jin S, Zhang N, Deng W, Seo MH, Wang X. Efficient Zn metal anode enabled by O,N-codoped carbon microflowers. *Nano Lett* 2022;22:1350-7. DOI PubMed